Dependence of stage-I recovery on the irradiation direction in copper doped with beryllium

A. C. Baily*
Materials Science Division, Argonne National Laboratory, Argonne, Illinois 60439
and Department of Materials Science and Engineering, Northwestern University, Evanston, Illinois 60208

W. E. King,† and K. L. Merkle
Materials Science Division, Argonne National Laboratory, Argonne, Illinois 60439

M. Meshii
Department of Materials Science and Engineering, Northwestern University, Evanston, Illinois 60208
(Received 17 June 1992)

Electron irradiations of thin Cu-Be films near displacement threshold show that the types of Frenkel pairs produced depend on recoil direction. Irradiation along ⟨100⟩ very strongly favors the production of close pairs that anneal in substages I_A and I_B, whereas irradiation along ⟨110⟩ produces mostly substage I_C close pairs. Substage I_D indicates the recombination of mobile defects; the larger Frenkel pair separation due to far-reaching replacement collision sequences along ⟨110⟩, as opposed to ⟨100⟩, is reflected in a shift of the peak recovery rate to higher temperature.

Point-defect production, recovery kinetics, and energy dependence of defect recovery after low-temperature electron irradiation of copper has long been studied.[1] Nevertheless, only a few stage-I recovery spectra using single crystals have been reported in the literature.[2–4] These experiments have shown that there are changes in the stage-I recovery spectrum with irradiation direction. However, the true extent of these changes has been masked due to multiple scattering of the irradiating electron beam in the thick specimens that were employed in these experiments. The present experiments circumvent this problem by using thin-film targets and the highly collimated, monoenergetic, electron beam available in a high-voltage electron microscope (HVEM). This technique allows further insight into defect production mechanisms and properties of irradiation-induced point defects.

The importance of multiple scattering in defect production can be understood by referring to the threshold energy surface determined by King, Merkle, and Meshii.[5] This threshold energy surface is characterized by two regions of low threshold energy ($\sim$20 eV) around the ⟨100⟩ and ⟨110⟩ directions, with the remaining directions being relatively high in threshold energy ($>$50 eV). Near-threshold electron irradiations, such as with 500 keV electrons, only produce stable defects by recoils along the two close-packed directions ⟨100⟩ and ⟨110⟩.[5] Irradiation with 500 keV electrons exactly along ⟨110⟩ produces Frenkel pairs only by lattice atom recoils along ⟨110⟩.[6] It can be shown, however, that as little as 10° of angular dispersion—due to multiple scattering—in electron irradiations along ⟨110⟩ will result in production of defects by atom recoils along ⟨100⟩. In previous experimental works[2–4] specimens >10 μm in thickness were used, which, for 500 keV electrons, results in $>15°$ of beam spreading,[3] thus obscuring the true anisotropy of defect production.

Multiple-scattering effects were minimized in the present work by using thin-film samples. The specimens were typically $\sim$0.5 μm thick. At this thickness the angular dispersion due to multiple-electron scattering is negligible in copper at 500 keV.

Thin copper films with low concentrations of beryllium atoms, such as used for studies of defect production at temperatures in stage II (Ref. 6) were prepared. The films were epitaxially grown on single-crystal rocksalt substrates by means of electron-beam evaporation of a bulk copper alloy containing $\sim$700 ppm Be at a deposition pressure of better than 3×10^{-6} Pa. The resulting thin films contained $\sim$100 ppm of beryllium atoms as deduced from the slope of the reciprocal damage rate at 55 K.[7] Secondary-ion mass spectroscopy showed that the beryllium distribution throughout the sample was uniform. The method of producing the specimen shape and specimen mounting procedures are described elsewhere.[8] The specimens were flat to 1.5° over the 0.1-mm gauge length used in the irradiations.

All experiments were performed using a side-entry type, single-tilt cryogenic specimen stage for use in the Kratos 1.2 MeV EM7 HVEM at Argonne National Laboratory (ANL). This He-flow cryostat allowed the adjustment of specimen temperatures between room temperature and less than 10 K with a temperature stability of better than 0.05 K. During irradiation the sample temperature was maintained below 10 K.

The ANL-HVEM provided a parallel electron beam at energies continuously adjustable between 100 and 1200 kV. During irradiation, the irradiating electron beam was monitored and maintained spatially uniform to within 1%. Sample orientation was precisely aligned to within 0.1° by means of Kikuchi electron diffraction at 100 kV. All resistivity measurements were made at temperatures less than 10 K and corrected for the electrical size effect.[9] We note that, since only fractional recoveries

are considered, possible errors due to the electrical size effect are negligible. The irradiation-induced defect concentration (<20 ppm) was less than the beryllium dopant atom content in each experiment. Following irradiation, recovery curves were obtained by annealing isochronally through stage I in 1.5 K steps with a holding time of 10 min.

The isochronal annealing data in Fig. 1 clearly show a strong dependence of stage-I recovery with irradiation direction. The corresponding recovery spectra in Fig. 2 even more graphically illuminate the changes in substage population with irradiation direction. Defect recovery after near-threshold irradiation was determined in several specimens (see Table I) and for three irradiation directions: along ⟨100⟩, along ⟨110⟩, and along a direction $\sim 10°$ from ⟨110⟩ toward ⟨100⟩ (see insets to Figs. 1 and 2). The irradiation-induced resistivity which remained after an anneal of ~ 12 h at room temperature was considerably smaller than the initial residual resistivity of the specimen.

Figures 1 and 2 clearly show strongly pronounced annealing peaks at 17 K (stage I_A) and 28 K (stage I_B) for the sample irradiated in the ⟨100⟩ direction. These peaks are almost completely suppressed in the sample irradiated along ⟨110⟩, indicating that at least one type of defect produced by recoils along ⟨100⟩ is practically absent when the recoil direction is ⟨110⟩. Conversely, stage I_C (32 K) is rather weak in ⟨100⟩ irradiations, compared to irradiation along ⟨110⟩. This suggests that the close-pair stage I_C is largely characteristic for defects produced by recoils in the ⟨110⟩ direction. A quite remarkable effect is the observed variation in peak position for stage I_D as a function of recoil direction. This has never been observed before, although stage I_D has in the past been ascribed to correlated recombination, i.e., the recombination by long-range migration of an interstitial with its own vacancy. Thus, the peak recovery temperature would be expected to depend on the number of long-range diffusional jumps necessary before recombination. Apparently, the separation distances of the defects produced in ⟨100⟩ and ⟨110⟩ irradiations are sufficiently different to cause a shift in peak temperature of about 2 K. We note here that the radiation-induced defect concentration was smaller than the number of Be traps. Hence, interstitial clustering and recombination of interstitials with vacancies other than their own can be neglected. The effect on the resistivity when an interstitial gets trapped at a Be site is not known; however, it is likely that there is only a small change (i.e., it can be assumed that the resistivities are additive). In this event, the much lower resistivity increment remaining after ⟨100⟩ irradiation in contrast to the ⟨110⟩ irradiation (see Fig. 1) also is a clear indication that the interstitials and vacancies are separated by noticeably shorter distances when irradiating in the former direction.

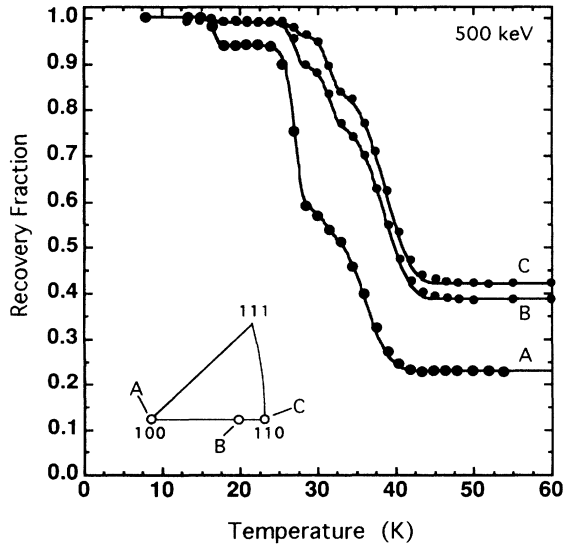

FIG. 1. Isochronal annealing curves of Be-doped, single-crystal Cu films. Stage-I recovery from near-threshold irradiation (500 keV) is shown for three irradiation directions, identified in the inset.

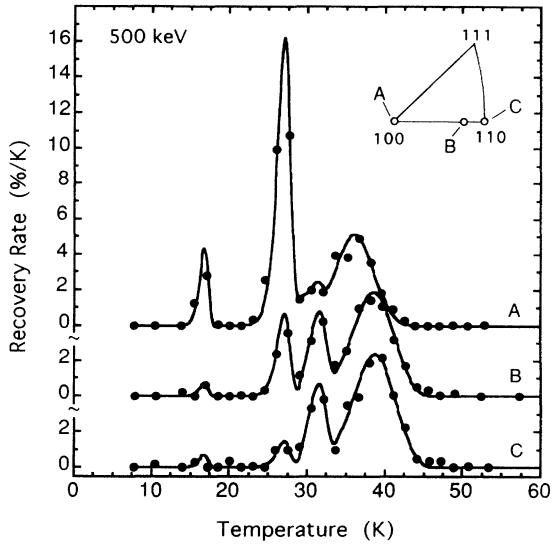

FIG. 2. Stage-I recovery rates from the electron irradiations in Fig. 1. The irradiation directions are shown in the inset.

In order to estimate the defect population of each substage—I_A, I_B, I_C, and I_D—the recovery data were analyzed in terms of simple recovery models. The recovery in the close-pair substages—I_A, I_B, and I_C—was calculated using first-order recovery kinetics.[10] Correlated recovery during long-range migration—substage I_D—was calculated using the high trap density approximation, with a modified exponential defect distribution, of Simpson and Sosin.[11] Substage I_E recovery was neglected because the presence of the beryllium interstitial traps suppresses virtually all of the recombination of interstitials with vacancies other than their own.[12] The values used for the activation energies and vibrational frequencies were obtained from previous work.[10,11] Substage populations were adjusted until a good eye fit was obtained with both the recovery and recovery-rate curves of the experimental data. Calculated recovery is represented in Figs. 1 and 2 by the solid lines. Substage populations obtained from the fits are given in Table I.

From Table I the amount of recovery in each substage

TABLE I. Stage-I recovery in Cu from near-threshold irradiations. Experiments were performed on five different specimens indicated by capital letters in column 1. $\Delta\rho_0$ is the irradiation-induced resistivity before anneal. I_{cp} is the fraction of defects in close-pair stages. f_{corr} is the fraction of freely migrating defects which recombine correlatedly.

			Fraction in substage						
Expt.	E (keV)	$\Delta\rho_0$ (nΩ cm)	I_A	I_B	I_C	I_D	I_{cp}	f_{corr}	Direction
*A*1	500	1.7	0.008	0.05	0.09	0.85	0.15		⟨110⟩
*B*1	500	1.9	0.072	0.32	0.075	0.53	0.47		⟨100⟩
*B*2	500	2.6	0.070	0.37	0.06	0.50	0.50		⟨100⟩
*C*1	500	5.1	0.060	0.34	0.04	0.56	0.44		⟨100⟩
*C*2	500	5.3	0.010	0.10	0.10	0.79	0.21		≈⟨110⟩[a]
*C*3	500	5.6	0.010	0.03	0.10	0.87	0.14		⟨110⟩
*D*1	500	4.9	0.0	0.06	0.07	0.87	0.13		⟨110⟩
*E*1	460	5.0	0.003	0.005	0.13	0.87	0.13		⟨110⟩
Average			0.067	0.343	0.058	0.53	0.47	0.58	⟨100⟩
Average			0.005	0.036	0.098	0.865	0.138	0.51	⟨110⟩

[a]10° off ⟨110⟩ toward ⟨100⟩.

for irradiations along the two close-packed directions can be compared. Irradiation along ⟨100⟩, as compared to irradiation along ⟨110⟩, greatly favors the formation of defects, which will recombine in a close-pair substage by a factor of $\simeq 3$. Atom recoils along ⟨100⟩ are ~ 13 times as likely to produce a substage I_A defect as a recoil along ⟨110⟩. Similarly, substage I_B is enhanced by a factor of $\simeq 10$ by irradiating along ⟨100⟩ instead of ⟨110⟩. Substage I_C is the only close-pair substage that is favored by irradiation along ⟨110⟩ instead of ⟨100⟩.

It would appear highly desirable to establish the correlation between the atomic structure of the close-pair defects and the observed I_A, I_B, and I_C substages. This could be attempted on the basis of results from molecular-dynamics calculations.[13] Selection of sites could be made by comparing the observed substage recovery fractions with the frequency of occurrence of a particular Frenkel pair configurations, as determined by molecular-dynamics calculations. At present no sufficiently detailed calculations are available to make such assignments. It seems likely, however, that substage I_A interstitials (which have the smallest activation energy) are located just outside the static recombination volume, V_0, along a direction toward ⟨100⟩, while I_C interstitial would be expected farthest away from their vacancy, in a direction at or near ⟨110⟩. Interstitials recombining in substage I_B may be of an intermediate distance. Since not even the topology of the spontaneous recombination volume is known in detail, no specific guesses of the possible Frenkel pair configurations can be made without detailed computer simulations.

It is remarkable, however, that in view of the relatively large surface area of the spontaneous recombination volume, the annealing spectrum is quite simple, especially for ⟨100⟩ recoils. This must be a consequence of the displacement process, which apparently near threshold allows only a very select set of defect configurations to survive the dynamics of Frenkel pair formation. One should add, however, that the interstitials annealing in stage I_D must have a range of configurations relative to their vacancy. Also, as the irradiation energy is increased, the multitude of possible defect configurations increases due to (i) the increased recoil energy, as well as due to (ii) the increase in available recoil directions for the same electron-beam direction.

The populations of substages I_B and I_C increase appreciably as the irradiating electron energy is lowered toward the threshold energy. This observation is consistent with the creation of defects by low-energy recoils along a close-packed direction. On the other hand, the population of substage I_A decreases with decreasing recoil energy. This suggests that in stage I_A close-pair defects are created at somewhat larger energy than the minimum threshold and for recoil directions deviating from the two favored close-packed directions.

Table I shows that even irradiations near threshold produce large numbers of defects which are not in close-pair configurations. At sufficiently high temperatures (~ 35 K in Cu, in substage I_D) these interstitials can undergo long-range migration. For near-threshold irradiations along ⟨100⟩ or ⟨110⟩, more than 50% of the interstitials produced can freely migrate.

In Fig. 2, it can be seen that the substage I_D recovery-rate peak occurs at a temperature a few degrees higher for irradiation along ⟨110⟩ than ⟨100⟩. In fcc materials the ⟨110⟩ direction is more closely packed than ⟨100⟩ and therefore more efficient in the mass and energy transfer by replacement collision sequences, resulting in larger Frenkel pair separations. For a simple three-dimensional random-walk model, the probability for correlated recovery is given by $f_{corr}=r_v/r_p$, where r_p and r_v are the average interstitial-vacancy separation and the effective recombination radius, respectively.[11] From Table I, assuming a spherical recombination volume and three-dimensional diffusion, we have $r_p^{\langle 110\rangle}/r_p^{\langle 100\rangle}\simeq 1.14$. Thus, interstitials produced by recoils along ⟨110⟩ will require more jumps on the average before they can annihilate with their vacancies, hence, the peak recovery

rate is shifted to a higher temperature.

In summary, a direct connection between the defect production process, including its anisotropy, and certain Frenkel pair configurations has been shown for the first time by using the thin-film technique of *in situ* low-temperature electron irradiation in the HVEM. A substantial fraction of the defects becomes mobile in stage I_D and the dependence of the spatial separation between vacancy and interstitial is reflected in a shift of this annealing peak, a variation which can be effected by selectively choosing suitable recoil directions. Further studies using this technique hold considerable promise in elucidating Frenkel pair production and point defect properties, especially when combined with detailed computer simulations and experimental variations involving studies of energy and directional dependencies near the displacement threshold.

The authors gratefully acknowledge the technical support of the Argonne National Laboratory High Voltage Electron Microscope-Tandem Facility and crew. This work has been supported by the National Science Foundation under Grant No. DMR-8114845 and by the U.S. Department of Energy, Basic Energy Sciences, Materials Science, under Contract No. W-31-109-Eng-38. The SIMS analysis of the Cu (Be) thin films was carried out in the Center of Microanalysis of Materials, University of Illinois-Urbana, which is supported by the DOE under Contract No. DE-AC02-76ER01198.

---

*Present address: 161 Sulgrave, Sterling, VA 22170.

†Present address: Lawrence Livermore National Laboratory, Livermore, California 94550.

[1]W. Schilling, G. Burger, K. Isebeck, and H. Wenzl, in *Vacancies and Interstitials in Metals,* edited by A. Seeger, D. Schumacher, W. Schilling, and J. Diehl (North-Holland, Amsterdam, 1970), p. 255.

[2]Y. Cusson, P. Lucasson, and R. M. Walker, in *Proceedings of The International Conference on the Properties of Reactor Materials,* edited by D. J. Littler (Butterworths, London, 1962), p. 92.

[3]A. Sosin, and K. Garr, Phys. Status Solidi **8**, 481 (1965).

[4]A. B. Pruitt and R. L. Chaplin, Radiat. Eff. **11**, 119 (1971).

[5]Wayne E. King, K. L. Merkle, and M. Meshii, J. Nucl. Mater. **117**, 12 (1983).

[6]A. C. Baily, W. E. King, K. L. Merkle, and M. Meshii, in *Advanced Photon and Particle Techniques for the Characterization of Defects in Solids,* edited by J. B. Roberto, R. W. Carpenter, and M. C. Wittels, MRS Symposia Proceedings No. **41** (Materials Research Society, Pittsburgh, 1985), p. 43.

[7]A. Bartels, J. Bewerunge, F. Dworschak, and H. Wollenberger, J. Phys. F **12**, 641 (1982).

[8]Wayne E. King, K. L. Merkle, and M. Meshii, Phys. Rev. B **23**, 6319 (1981).

[9]E. H. Sondheimer, Adv. Phys. **1**, 1 (1952).

[10]J. W. Corbett, R. B. Smith, and R. M. Walker, Phys. Rev. **114**, 1542 (1959).

[11]H. M. Simpson and A. Sosin, Radiat. Eff. **3**, 1 (1970).

[12]A. Sosin and H. H. Neely, Phys. Rev. **127**, 1465 (1962).

[13]Wayne E. King and R. Benedek, in *Proceedings of Point Defects and Defect Interactions in Metals,* edited by J. Takamura, M. Doyama, and M. Kiritani (University of Tokyo Press, Kyoto, 1982), p. 807.